ELSEVIER

Thermochimica Acta 400 (2003) 1–20

thermochimica acta

www.elsevier.com/locate/tca

Aggregation and gelation of divalent cell surface receptors by rigid polyvalent ligands: examination by theoretical, kinetic and thermodynamic techniques☆

B. George Barisas*

Departments of Chemistry and Microbiology, Colorado State University, Fort Collins, CO 80523, USA

Received 10 September 2001; received in revised form 11 July 2002; accepted 17 July 2002

Abstract

Various cell surface proteins, such as the B cell receptor (BCR) or immunoglobulin E bound to the membrane Type I Fcε receptor, possess two or more binding sites for soluble ligands which in turn have valences of three or more. We have devised an equilibrium model to calculate sizes and structures of cell surface aggregates formed between such species in two-dimensional systems directly from solution ligand concentration. The model explicitly treats differing ligand valences for different types of receptor-binding, monogamous bivalent binding of ligand-to-receptor and two-dimensional gelation of receptor–ligand aggregates. Of particular interest is that thermodynamic parameters reasonable for cell biological situations predict that two-dimensional receptor gelation can occur. This is the appearance of large aggregates (gel) in equilibrium with appreciable amounts of finite-sized aggregates (sol). Calculations also suggest (1) the amount of bound ligand increases with ligand concentration or ligand valence below the gel point, (2) the average number of receptors per finite aggregate increases with ligand concentration below the gel point, (3) finite aggregates generally involve less than two ligand molecules, (4) above the gel point, finite aggregate size remains approximately constant and bound ligand enters the gel-phase. Predicted gelation is also consistent with experiment. Polyvalent dinitrophenyl (DNP) antigens can aggregate bivalent DNP-specific BCR on cell or liposome surfaces. We have used the laser-microscopic method of fluorescence photobleaching recovery to examine the mobility of such protein aggregates both on B cells bearing DNP-specific BCR and on liposomal models. When either the DNP-antigen solution concentration or the number of DNP groups per antigen molecule exceeds a critical value, a fraction of the normally mobile bound antigen becomes immobile. At the same time, cells become resistant to antigenic and mitogenic stimulation. This suggests that two-dimensional gelation of antigen and BCR occurs with inhibition of subsequent BCR function. We discuss possible mechanisms by which large, immobile protein aggregates might inhibit cellular signaling systems, for example by slowing translocation of liganded receptor to lipid rafts.

Keywords: Antigen; Precipitin; B cell; Mast cell; Immunoglobulin

1. Introduction

Various cell surface proteins, such as the B cell receptor (BCR) or immunoglobulin E bound to membrane Fcε receptors, possess two or more binding sites for soluble ligands which in turn have valences of three or more. The binding of ligands—antigens, allergens,

Abbreviations: BCR, B cell receptor or membrane immunoglobulin; DNP, 2,4-dinitrophenyl; LUV, large unilamellar vesicles; POL, polymerized flagellin from *Salmonella adelaide*; TI, thymus-independent

☆ This paper was part of the ISBC XII Proceedings.

* Tel.: +1-970-491-6641; fax: +1-970-491-1801.
E-mail address: barisas@lamar.colostate.edu (B. George Barisas).

0040-6031/03/$ – see front matter © 2002 Elsevier Science B.V. All rights reserved.
PII: S0040-6031(02)00403-3

Nomenclature

C	molar concentration of ligand molecules in solution
C^*	vK_1C
C_{kij}	cell surface concentration of aggregates involving k ligand molecules and i receptors, j of which are bound monogamous bivalently
f	number of determinants per ligand molecule capable of simultaneously binding to receptors not bound to other ligand molecules
h	number of determinants per ligand molecule capable of simultaneous involvement in inter-ligand crosslinks by receptors
K_1	binding constant for the interaction of a site on a free receptor with a determinant on an ligand molecule free in solution
K_2	binding constant for a ligand determinant, on a ligand already attached to the cell surface, binding to a receptor site
K_3	binding constant for the interaction of a site on a receptor molecule, already bound to ligand at its other site, with an ligand determinant on a *different* ligand molecule
K_4	binding constant for the interaction of a site on a receptor molecule already bound to ligand at its other site with a ligand determinant on the same molecule
r	K_3/K_2
R_{kij}	number of ways i receptors can be employed to join k ligand molecules and then bind remaining available ligand sites
S	concentration of free cell surface receptors
S^*	$2K_2S$
v	number of determinants per ligand molecule capable of *initial* attachment to a cell surface receptor
W_k	number of ways k ligand molecules can be assembled into an aggregate
W_{kij}	number of ways an aggregate of k ligands and i receptors, of which j are bound monogamous bivalently, can be formed

etc.—to such cell surface receptors is thus the primary event in triggering several significant classes of biological responses. The sizes of receptor–ligand complexes formed under various conditions has long been recognized as a determinant of the type and magnitude of cellular responses resulting from ligand encounter.

The equilibrium thermodynamics of such complex aggregating systems have been examined theoretically and experimentally over many years. In studying polymerization reactions, Stockmayer [1] developed many of the combinatoric tools need for modeling such processes, proceeding from a formalism developed by Mayer and Mayer [2]. Goldberg specifically examined the case of antibody–antigen aggregation in solution [3]. A common feature of both these studies was the recognition of gelation in aggregating systems, namely the sudden appearance of an arbitrarily large aggregate in equilibrium with finite-sized species. More recently, individuals such as Perelson [4], DeLisi [5], Baird et al. [6] and Goldstein et al. [7] have examined the interaction of rigid, polyvalent antigen with cell surface receptors. These various treatments have considered, with enormous sophistication, factors affecting aspects of aggregation, measures of receptor crosslinking, kinetic approaches to equilibrium, monogamous bivalent binding of receptors to individual ligands and possibilities for critical phenomena like gelation. However, these treatments have generally not been suited to predicting experimental results directly from model parameters and experimental conditions.

This paper develops a computational model for the equilibrium binding of a rigid polyvalent ligand to divalent cell surface receptors in terms of total external ligand concentrations. The model explicitly treats differing ligand valences for different types of receptor-binding, monogamous bivalent binding of ligand-to-receptor and two-dimensional gelation of receptor–ligand aggregates.

While the model presented is applicable to any divalent receptor and polyvalent ligand, we will frequently refer to the one particular system, namely the binding of DNP–POL antigen to DNP-specific receptors on B lymphocytes. Antigen concentration effects both on the in vitro antigenicity of DNP–flagellin and on lateral mobilities of receptor–antigen aggregates demonstrate a complex dependence of antigen–receptor aggregate structure on antigen concentration and valence. This suggests that structure of receptor–antigen aggregates formed under different conditions can vary widely and that aggregate structure is a strong determinant of biological effect. Moreover, both cell and model systems give clear indication of the appearance of a gel-phase under some but not all conditions associated with cellular function.

Together with measured or estimated thermodynamic parameters for such aggregation processes, the model is used to calculate various parameters of receptor aggregation phenomena under specific experimental conditions examined for DNP–POL antigen binding to DNP-specific receptors on B lymphocytes examined in studies previously noted [8–11]. Quantitative predictions of the model are compared with various biophysical data obtained on these actual cell surface aggregation processes.

2. Theory

2.1. Derivation of the model

The question at hand is as follows: given bivalent receptors confined to a cell surface and rigid, polyvalent ligand molecules, such as antigen or allergen, in solution, what receptor–ligand complexes are present on the cell surface at equilibrium? A suitable form of answer is per-cell concentration C_{kij} of aggregates involving i molecules of receptor and k molecules of ligand. In general, there may be some monogamous binding of receptors to the same ligand molecule. $j \leq i - k + 1$ denotes the number of receptors so bound. Such problems can be treated by Stockmayer's combinatoric methods [1] or by probabilistic approaches derived subsequently to circumvent various difficulties [12]. We choose the first approach because of its greater conceptual simplicity.

Our system involves four types of ligand–receptor bonds (Fig. 1) and the ligand exhibits three valences, each appropriate to various bond types. The first type of bond, denoted by subscript 1, is the initial binding of ligand to the cell surface. If the ligand has v reactive groups (antigenic determinants) present on its surface, each is potentially capable of forming this first bond to a cell surface receptor. The intrinsic binding constant

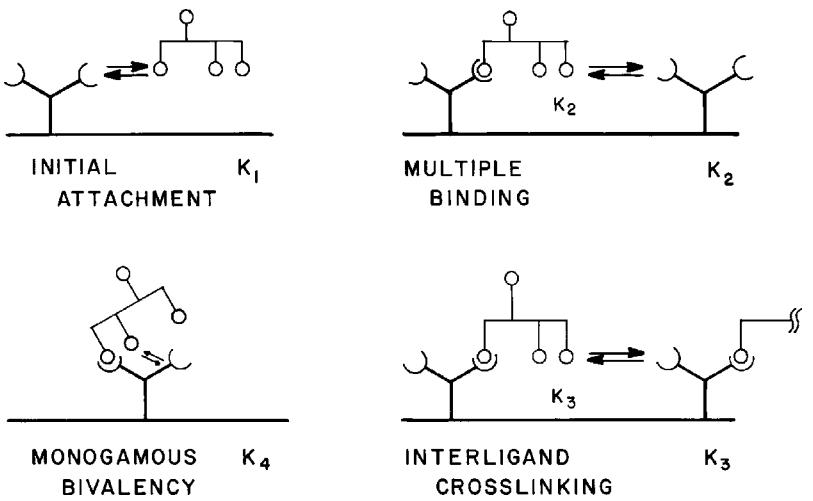

Fig. 1. Modes of interaction between multivalent ligand and bivalent cell surface receptors. The number of ligand sites capable of interacting through the first mode, i.e. initial attachment, is v. Interaction through the second mode, i.e. a free receptor plus an already bound ligand, is possible at f sites. Inter-ligand crosslinking is possible at h sites. Solution ligand concentration affects only the first binding step.

and free energy of this interaction are K_1 and ϵ_1. Once a ligand is anchored to the cell surface, only $f \leq v$ functional groups can bind receptors at the same time. In particular, some groups may extend away from the cell surface and thus be unavailable for surface receptor interactions. The intrinsic binding constant and free energy of these bonds are K_2 and ϵ_2. Next, $h \leq f$ groups on a bound ligand are capable of bridging via a bivalent receptor to another bound ligand. Such binding has an intrinsic equilibrium constant and free energy K_3 and ϵ_3. Finally, if a sIg bound to one site on the antigen binds monogamously to a second site on the same antigen molecule, the intrinsic binding constant and free energy for this interaction are K_4 and ϵ_4, respectively. Consider the formation of a mole of *kij*th aggregate from k moles ligand in solution and i moles of free cell surface receptor. This process involves the formation of k bonds of the first type, $i-k$ bonds of the second type, $k-1$ bonds of the third type and j bonds of the fourth type. The standard molar free energy ΔG°_{kij} of the process is given by

$$\Delta G^{\circ}_{kij} = k\varepsilon_1 + (i-k)\varepsilon_2 + (k-1)\varepsilon_3 + j\varepsilon_4 - RT\,\ell n\left(\frac{W_{kij}}{k!i!}\right) \quad (1)$$

where W_{kij} is the number of ways the k ligands and i receptors can be arranged to form the *kij*th aggregate. The equilibrium constant K_{kij} for the reaction is therefore

$$K_{kij} = \exp\left(-\frac{\Delta G_{kij}}{RT}\right) = K_1^k K_3^{k-1} K_2^{i-k} K_4^j \frac{W_{kij}}{k!i!} \quad (2)$$

The per-cell concentration C_{kij} of the *kij*th species is then given by

$$C_{kij} = K_{kij} C^k S^i \quad (3)$$

where C and S are, respectively, the free ligand and free receptor concentrations.

Appendix A shows how W_{kij} can be evaluated in analogy with the procedures of Goldberg [3] and of DeLisi and Perelson [12]. The result is given as

$$W_{kij} = \eta\, i!\, 2^i v^k \frac{(hk-k)!}{(hk-2k+2)!}\frac{(n-j)!}{j!(n-2j)!} \times \frac{(n-2j)!}{q!(n-2j-q)!} \quad (4)$$

where η is approximated by $(h-1)/(f-1)$, $n = fk-2k+2$ is the number of antigen sites *not* involved in the $k-1$ inter-antigen bridges and $q = i-k+1-j$ is the number of singly-bound receptors. It is convenient to define $r = K_3/K_2$ and to replace K_3 by rK_2. Combining Eqs. (3) and (4) and making the indicated substitution, we get

$$C_{kij} = \eta k_2^{-1} (vK_1C)^k r^{k-1} (2K_2S)^i K_4^j \times \frac{(hk-k)!}{k!(hk-2k+2)!}\frac{(n-j)!}{j!(n-2j)!} \times \frac{(n-2j)!}{q!(n-2j-q)!} \quad (5)$$

If S_0 denotes the total number of receptors on the cell surface, then conservation of receptors is expressed by the equation

$$S_0 = \sum iC_{kij} + S. \quad (6)$$

2.2. Summation of the distribution function

The problem remaining is to find practical methods of evaluating the distribution function C_{kij} and its derivatives with respect to k, i and j. These quantities permit Eq. (6) to be solved for S when a value of C is specified. The distribution of species C_{kij} can then be calculated.

If we sum Eq. (5) over all possible values of k, i, and j, we obtain

$$\sum C_{kij} = \frac{\eta}{rK_2S^*}\sum_{k=1}^{\infty}\frac{(hk-k)!}{k!(hk-2k+2)!}(rC^*S^*)^k \times \sum_{j=0}^{\mathrm{int}(n/2)}\frac{(n-j)!}{j!(n-2j)!}(K_4S^*)^j \times \sum_{q=0}^{n-2j}\frac{(n-2j)!}{q!(n-2j-q)!}(S^*)^q \quad (7)$$

where $C^* = vK_1C$ and $S^* = 2K_2S$. This sum includes $C_{100} = C$, the free ligand concentration in solution. Since this species is not bound to the cell surface, we will not want to consider it in estimating average properties of bound aggregates. Rather than attempting to change the limits of summation, we will henceforth subtract C from all sums where the term appears at the time of use.

The sum over q is simply evaluated by the binomial theorem:

$$\sum C_{kij} = \frac{\eta}{rK_2S^*}\sum_{k=1}^{\infty}\frac{(hk-k)!}{k!(hk-2k+2)!}(rC^*S^*)k \times(1+S^*)^{fk-2k+2}\sum_{j=0}^{\mathrm{int}(n/2)}\frac{(n-j)!}{j!(h-2j)!} \times\left[\frac{K_4S^*}{(1+S^*)^2}\right]^j = \frac{\eta(1+S^*)^2}{rK_2S^*}\sum_{k=1}^{\infty} \times\frac{(hk-k)!}{k!(hk-2k-2)}[rC^*S^*(1+S^*)^{f-2}]^k \sum_{j=0}^{\mathrm{int}(n/2)}\frac{(n-j)!}{j!(h-2j)!}\frac{K_4S^*}{(1+S^*)^2} \quad (8)$$

The sum over j can also be evaluated in closed form using a known combinatoric relation [13]:

$$\sum_{j=0}^{\mathrm{int}(n/2)}\frac{(n-j)!}{j!(n-2j)!}z^j = \xi^{n/2}\frac{1+(-1)^n\zeta^n}{1+\zeta} \quad (9)$$

where

$$z = \frac{K_4S^*}{(1+S^*)^2} \quad (9a)$$

$$x = 1+2z+(1+4z)^{1/2} \quad (9b)$$

$$\xi = \tfrac{1}{2}x \quad (9c)$$

$$\zeta = \frac{2z}{x} \quad (9d)$$

Since $0 \le \zeta < 1$ this formulation of the sum is extremely well-behaved for computational purposes. The main sum then becomes

$$\sum C_{kij} = \frac{(1+S^*)^2}{rK_2S^*}\left[\frac{\xi}{1+\zeta}\sum_{k=1}^{\infty}\frac{(hk-k)!}{k!(hk-2k+2)!}y_0^k + \frac{\xi\zeta^3}{1+\zeta}\sum_{k=1}^{\infty}\frac{(hk-k)!}{k!(hk-2k+2)!}y_1^k\right] \quad (10)$$

where

$$y_0 = rC^*S^*[\xi^{1/2}(1+S^*)]^{f-2} \quad (10a)$$

$$y_1 = rC^*S^*[-\xi^{1/2}\zeta(1+S^*)]^{f-2} \quad (10b)$$

The above sums are of a type evaluated by Stockmayer some years ago [1]. If one defines

$$T_i = \sum_{k=1}^{\infty}k^i\frac{(hk-k)!}{k!(hk-2k+2)!}y^k \quad (i=0,1) \quad (11)$$

Then

$$T_0 = \frac{\alpha(1-\alpha h/2)}{(1-\alpha)^2h} \quad (12)$$

and

$$T_1 = \frac{\alpha}{(1-\alpha)^2h} \quad (13)$$

In the previous equations, α is defined implicitly as the smallest positive root of

$$y = \alpha(1-\alpha)^{h-2} \quad (14)$$

The computational formula for $\sum C_{kij}$ thus becomes

$$\sum C_{kij} = \frac{\eta(1+S^*)^2}{rK_2S^*} \times\left[\frac{\xi}{1+\zeta}T_0(y_0)+\frac{\xi\zeta^3}{1+\zeta}T_0(y_1)\right] \quad (15)$$

It is now clear how $\sum C_{kij}$ is to be computed. When S^* is known or assumed, the power series variables y_0 and y_1 may be calculated from the definitions of Eqs. (10a) and (10b). Eq. (14) is then solved for α_0 and α_1, the solutions corresponding to y_0 and y_1. Insertion of these quantities into Eq. (10) yields $T_0(y_0)$ and $T_0(y_1)$ and C_{kij} stands explicitly evaluated from Eq. (15).

The sum representing the amount of bound ligand $\sum kC_{kij}$ can be computed without additional effort. Consideration of Eqs. (10), (11) and (13) shows that

$$\sum kC_{kij} = \frac{\eta(1+S^*)^2}{rK_2S^*} \times\left[\frac{\xi}{1+\zeta}T_1(y_0)+\frac{\xi\zeta^3}{1+\zeta}T_1(y_1)\right] \quad (16)$$

Once α_0 and α_1 are known, $T_1(y_0)$ and $T_1(y_1)$ follow trivially from Eq. (13).

As was stated earlier, the fundamental problem of this computation is to evaluate the free receptor concentrations given a fixed value for the solution ligand concentration C. The desired value of

S is that which solves Eq. (6). For such a solution, $\sum iC_{kij}$ must be evaluated and Eq. (5) in turn shows that

$$\sum iC_{kij} = S^* \frac{\mathrm{d}\sum C_{kij}}{\mathrm{d}S^*} \tag{17}$$

One should note that the sum includes only ligand bound receptors since the sum begins at $k = 1$. Thus, the average number of receptors $\langle i \rangle$ per aggregate and the average number of monogamous bivalently bound receptors $\langle j \rangle$ refer to ligand-binding receptors only. The preceding differentiation could clearly be accomplished numerically. However, in the interest of accuracy, it is advantageous to evaluate the sum exactly by analytically differentiating Eq. (10) and reapplying Stockmayer's formulae. The considerable algebra involved is set down in Appendix B. It matters here only that $\sum iC_{kij}$ can be evaluated explicitly for an assumed value of S.

If one examines Eq. (5) and considers the sum $\sum iC_{kij}$, it is clear without the necessity of formal proof that the sum is a monotonically increasing function of S. This fact permits Eq. (6) to be solved readily by successive approximations. A value may be assumed for S and the implied value S_0' for the total receptor concentration evaluated from Eq. (6):

$$S_0' = \sum iC_{kij} + S \tag{18}$$

If S_0' exceeds S_0, S must be reduced and S_0' recomputed. If S_0' is less than S_0, S must be increased before the next iteration. An interval bisection method is most efficient for the actual computation. If the initial value assumed for S is S_0, then $\log_2(S/S_0)$ iterations are required to establish the magnitude of S and m additional iterations suffice to evaluate S to a precision of one part in 2^m.

2.3. Properties of the distribution function

The main interest in the distribution function lies in various averages which can be calculated. The average number $\langle i \rangle$ of receptors per aggregate can easily be evaluated as

$$\langle i \rangle = \frac{\sum iC_{kij}}{\sum C_{kij} - C} \tag{19}$$

Here, we must subtract the $C_{100} = C$ term from the total species sum. The average number $\langle k \rangle$ of antigens per aggregate is similarly evaluated as

$$\langle k \rangle = \frac{\sum kC_{kij} - C}{\sum C_{kij} - C} \tag{20}$$

The $\sum kC_{kij}$ term is evaluated using Stockmayer's T_1 sum given in Eq. (13). Finally, the average number $\langle k \rangle$ of receptors bound monogamous bivalently given by

$$\langle j \rangle = \frac{\sum jC_{kij}}{\sum C_{kij} - C} \tag{21}$$

where

$$\sum jC_{kij} = \frac{\mathrm{d}\sum C_{kij}}{\mathrm{d}\,\ell n\, Z}$$

This sum is accompanied by considerable algebraic complexity; but, like the sum weighted by i, no new techniques are involved. The details of this differentiation are given in Appendix C. One should note that this particular sum cannot readily be evaluated by numerical differentiation of $\sum C_{kij}$.

The fundamental quantity obtained from fluorescence photobleaching recovery measurements of ligands bound to antigen-specific receptors on cells and liposomes [8–11] is the diffusion coefficient of bound ligand. For an extended aggregate, i.e. free draining with respect to other membrane species, the diffusion coefficient is inversely proportional to the number of receptors anchoring the aggregate to the membrane. Thus, the diffusion coefficient of a single receptor, divided by the diffusion coefficient of an aggregate, which we call the "mobility reduction index" M can be considered to approximate the number of receptors aggregated [14]. Limitations of this extremely simplified treatment, especially as it might apply to cells rather than liposomes, have been discussed elsewhere [15]. Since signals in photobleaching are weighted by the number of labeled ligands in an aggregate, this quantity is calculated from the model as

$$M = \frac{\langle ki \rangle}{\langle k \rangle} \tag{22}$$

The average $\langle ki \rangle$ is obtained by numerical differentiation of $\langle k \rangle$ with respect to $\ell n\, S^*$.

2.4. Gelation

The question of when, if ever, two-dimensional gelation occurs on the cell surface is of considerable interest. For trivalent ligands only, the matter has been examined in detail by Goldstein and Perelson [16]. Our generalized approach derives from Stockmayer's observation [1] that the sums T_0 and T_1 include only species present in finite-sized (sol-phase) aggregates. When a gel-phase namely an arbitrarily large aggregate, appears, it thus proves impossible to find a value of S which will make $\sum iC_{kij} + S$ as large as S_0. This situation arises because y_0 and y_1 both have a maximum value y_c of $(h-2)^{h-2}/(h-1)^{h-1}$. This critical value limits the number of sol-phase receptors which are enumerated by T_0. When no gel is present, Eq. (6) rapidly converges to a free receptor concentration which correctly predicts the total, i.e. bound and free, receptor concentration. Precisely at the onset of gelation, y_0, which is strictly larger than y_1, first becomes equal to y_c; nonetheless, Eq. (6) can satisfactorily be solved. Above the gel point, y_0 can still not exceed y_c. The minimum discrepancy between S_0' and S_0 results from a value of S which makes y_0 equal y_c. The value of S_0' at this time equals the number S_s of sol-phase receptors:

$$S_s = \sum iC_{kij} + S \tag{23}$$

The number of gel-phase receptor S_g is given simply by

$$S_g = S_0 - S_s \tag{24}$$

Finally, the fraction of receptors g_r in the gel-phase is given by

$$g_r = \frac{S_g}{S_0} \tag{25}$$

It is somewhat more difficult to resolve the relative amounts of antigen in the sol and the gel. The amount C_s of sol-phase bound ligand is easily obtained as

$$C_s = \sum kC_{kij} - C \tag{26}$$

The amount of gel-phase bound ligand is evaluated by considering the receptor–ligand ratio in aggregates with arbitrarily large values of k. In the limit of $k \to \infty$, this must approach the receptor–ligand ratio S_g/C_g in the gel. The result is given as

$$\frac{S_g}{C_g} = 1 + (f+2)\left[\frac{S^*}{1+S^*} + \frac{\xi'}{2\xi}\right] \tag{27}$$

Since S_g is already known, this defines C_g. The total bound ligand C_b is of considerable experimental interest and is given by

$$C_b = C_s + C_g \tag{28}$$

The fraction g_g of ligand in the gel is given by

$$g_\ell = \frac{C_g}{C_b}. \tag{29}$$

2.5. Two-dimensional constraints on aggregate structures

The above treatment of ligand–receptor aggregation cannot be directly applied to receptor aggregates with rigid, linear ligands constrained to a two-dimensional system. This is because Goldberg's combinatorics permit one antigen to be crosslinked via a receptor to another antigen at any points on each antigen molecule. In particular, two such linear ligands could be crosslinked from the middle of one to the middle of another. For a rigid antigen like DNP–POL, this is physically impossible in a two-dimensional system. A POL rod is about 120 Å in diameter [17], a dimension comparable to the diameter of a BCR complex. Thus, it is unlikely that two non-parallel ligands can be crosslinked middle to middle by a receptor which would have to be removed from the membrane to accomplish this. Thus, crosslinking can presumably occur only when the *end* of one rod abuts another rod at an arbitrary location. In other words, a valid branching point for the antigen lattice must involve at least one antigen rod end. This situation can be approximated numerically as follows. If an antigen has, among its valences accessible for crosslinking, a fraction f_e on ends, what is the probability that *two* crosslinked antigens are bridged with at least one end valence being used? This is simply one minus the probability that two medial valences are involved. Thus, for k ligands, $k-1$ crosslinks are involved and, to a first approximation, the probability P_k that an aggregate exists in three dimensions can also exist in the plane is simply given by

$$P_k = [1-(1-f_e)^2]^{k-1} = [2f_e - f_e^2]^{k-1} \tag{30}$$

To use this result in our calculation, we can simply define a new variable $r' = P_2 r$ to replace r in Eq. (5). The approximation used in this calculation should be reasonably accurate provided that too much receptor–ligand branching does not occur. As will be shown later, this seems to be the case in all physically-realistic situations.

3. Results

The calculations required to evaluate the model numerically were implemented in PowerBasic on PC-compatible computer. Values of C, v, f, h, S_0, K_1, K_2, R and K_4 were assumed at the outset of each calculation. The antigen concentration C was then varied from 10^{-16} to 10^4 M in half-decade steps. For each antigen concentration, the quantities S, C_b, $\langle k \rangle$, $\langle i \rangle$, $\langle j \rangle$, M, S_s/C_s, S_g/C_g, g_T, and g_r were evaluated by the formulae derived previously.

The equilibrium interaction of rigid polyvalent ligands with membrane receptors depends, according to our model, on nine separate physical parameters of which six are independent. As a practical matter, it is therefore, impossible to describe the effects of simultaneously varying all of these parameters. Our goal must therefore be more modest: to first describe the general features of binding for plausible values of the adjustable parameters and then to show how variation of one parameter at a time affects the observable properties of ligand–receptor interactions. Finally, we will suggest how the model helps interpret our photobleaching recovery results on lateral mobility of BCR–DNP–POL complexes on murine B cells and liposomes.

3.1. Model parameters relevant to cellular systems

Selection of values for the physical parameters permits considerable freedom of choice. We restrict our consideration here to DNP–polymerized flagellin, though the same numbers should be valid for DNP–dextran as well. In a recent study, polymerized flagellin exhibited an average length of about 1900 Å, corresponding to about 180 monomer units [18]. The *maximum* total valence of a DNP–POL molecule is thus about 200 times the epitope density.

We might expect that f and h would not exceed one-third the number of DNP groups conjugated onto a polymer. If the maximum attainable epitope density of DNP–polymerized flagellin is about 4, then $0 < f$, $h < 240$. A typical intrinsic binding constant of DNP-specific BCR for a DNP-protein is $5 \times 10^5\,\mathrm{l\,mol^{-1}}$ [18] and this can be equated to K_1. Optimum immunogenic responses often result from concentrations of about $1\,\mu\mathrm{g\,ml^{-1}}$ [15] and epitope densities of about 2 DNP per 40,000 Da flagellin monomer. Thus, in the region of interest to us, $C^* = vK_1C$ might have a value of about 0.01. Further, since v, K_1 and C occur only as the product C^*, we will simply plot this variable as our single effective concentration parameter.

Perhaps the most problematic quantities are K_2 and K_3. Theoretical consideration of crosslinking two bivalent antibodies with intrinsic affinities of $10^7\,\mathrm{l\,mol^{-1}}$ by 30–40 Å bivalent haptens predicts K_2 of about $10^{-9}\,\mathrm{cm^2}$ per molecule [19]. Typical BCR affinities for DNP are lower than this [18] at about $5 \times 10^5\,\mathrm{l\,mol^{-1}}$ and assuming 10^5 BCR per $200\,\mu\mathrm{m^2}$ cell leads to $K_2 \sim 2$. It has been suggested [16], and indeed seems plausible, that K_3 should be less K_2.

K_4 can be estimated given the spacing of ligand valences. From the geometry of POL rods [18], one can calculate a surface density of $6.2 \times 10^{12}\,\mathrm{DNP\,cm^{-2}}$ and an epitope density of 1 DNP per flagellin monomer. Assuming an intrinsic affinity of $5 \times 10^5\,\mathrm{l\,mol^{-1}}$ and that the second site of a receptor can explore a hemisphere of 15 Å radius, we estimate K_4 at 0.005 for an epitope density of one and so would not expect monogamous bivalent attachment to play a large role in our own experimental data. However, similar geometric arguments applied to the 15 or more DNP groups typically attached to bovine serum albumin or other carrier protein in studies of mast cell degranulation show that for these systems, K_4 values substantially *larger* that unity are to be expected. Thus, while monogamous bivalent receptor to ligand may not have strong relevance to our own BCR–DNP–POL experimental data, the phenomenon promises to have clear importance in other experimental systems to which the model applies.

3.2. Qualitative predictions of the model

Figs. 2–5 demonstrate qualitative aspects of receptor aggregation by ligands using sets of parameters

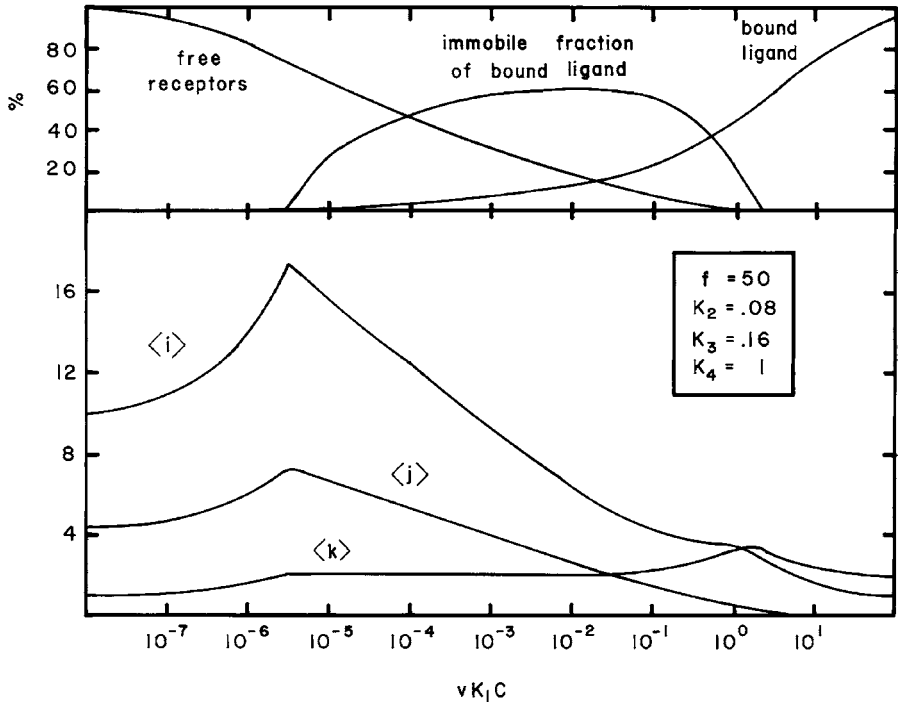

Fig. 2. Parameters of receptor aggregation calculated according to model. The parameters generating these data were not intended to represent a specific cellular situation but rather to demonstrate qualitative features of the model. For the calculation shown, f and h are both 50, K_2 is 0.08, K_3 is 0.16 and K_4 is 1. The x-axis is the dimensionless reduced concentration vK_1c. The upper panel shows the fraction of free receptors, the fraction of immobile, i.e. gel-phase, ligand and the fraction of total ligand bound for various reduced ligand concentrations. The actual limiting value for bound ligand is 2 per receptor. The lower panel shows the average numbers of receptors ($\langle i \rangle$), of monogamous bivalently bound receptors ($\langle j \rangle$) and of ligands ($\langle k \rangle$).

chosen to demonstrate these features. These parameters sets are not intended to necessarily represent cellular experiments or situations. Fig. 2 shows the ligand concentration of speciation while Table 1 provided the corresponding comprehensive tabulated output. Here, f and h are 50, K_2 and K_3 have values of 0.08 and 0.16, respectively and quite strong monogamous bivalent interaction is permitted ($K_4 = 1$). The upper part of the Fig. 2 shows that, as the ligand concentration increases, the fraction of free receptors declines, bound ligand increases, and the average size of receptor–ligand aggregates increases until the gel or critical point is reached. At this point, an immobile fraction of bound antigen (and bound receptors) appears, the average number of receptors $\langle i \rangle$ per mobile aggregate decreases slowly, and the number of antigens $\langle k \rangle$ per mobile aggregate remains constant at about 2. Finally, when high enough ligand concentrations are reached, the gel-phase disappears and, eventually, the average aggregate consists of one receptor and two ligands as one would intuitively expect. Table 1 shows that both sol and gel receptor–ligand ratios decrease monotonically with ligand concentration, the gel always exhibiting the higher numeric value. At very high ligand concentrations, sol receptor–ligand ratio approaches 0.5 since two ligand molecule bind each receptor.

A particularly important quantity is the average number $\langle i \rangle$ of receptors per aggregate. As calculated here and as noted earlier, both $\langle i \rangle$ and $\langle j \rangle$ average only ligand binding receptors. Thus, at low ligand concentrations where receptors are bound to single molecules, the average number of receptors per aggregate is some fraction of the total number of sites f per ligand, as determined by K_2. At higher ligand concentrations, aggregates grow through the recruitment

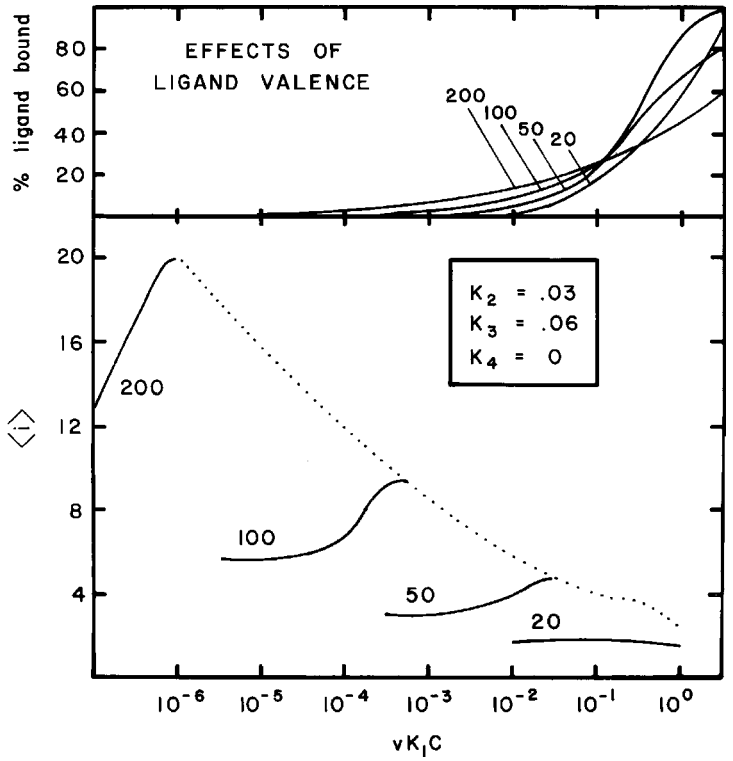

Fig. 3. Effects of ligand valence of receptor aggregation. The parameters generating these data were not intended to represent a cellular situation but rather to demonstrate qualitative features of the model. For the calculation shown, K_2 is 0.03, K_3 is 0.06 and K_4 is 0. The x-axis is the dimensionless reduced concentration vK_1c. The solid lines in the lower panel show $\langle i \rangle$ below the gel point for various values of f or, equally, h as indicated. Dotted lines indicate average size of sol-phase species *above* the gel point. The upper panel indicates total cell-bound ligand for the various ligand valences and concentrations.

of more ligands with their bound receptors. The largest average mobile aggregates occur at the gel point (Fig. 2) and sizes decrease at higher ligand concentrations. However, photobleaching recovery experiments measure signals in proportion to the number of *ligand* molecules so that average aggregate sizes inferred from such experiments are weighted by k. Thus, our mobility reduction index $\langle ki \rangle / \langle k \rangle$ most appropriately relates to photobleaching experiments.

What is most easily measured experimentally are effects of ligand concentration and valence (or epitope density) on system properties. Fig. 3 shows how the amount of bound ligand and the average number of receptors $\langle i \rangle$ per aggregate vary with these quantities. The various curves show calculations for f, $h =$ 20, 50, 100, and 200. The value of $\langle i \rangle$ increases both with ligand concentration and valence for all ligand shown. However, for antigens above their gel points, the variation in $\langle i \rangle$ with antigen valence is very small and cannot be seen on the graph. The upper part of Fig. 3 shows the predicted variation in total bound ligand with ligand concentration and valence. Both for cells in the range of physiological interest and for liposomal model systems, $vK_1c \sim 0.02$. In this range, Fig. 3 shows that the total amount of bound ligand increases with antigen concentration and valence.

Fig. 4 shows the effect of monogamous bivalency. The effect of increasing K_4 is to increase the avidity of the antigen for the cell surface so that saturation of available receptors occurs at lower and lower antigen concentrations and the gel point, indicated by the peak in the $\langle i \rangle$ curves, moves to lower and lower ligand concentrations. However, monogamous bivalency opposes multi-antigen aggregate formation so that the

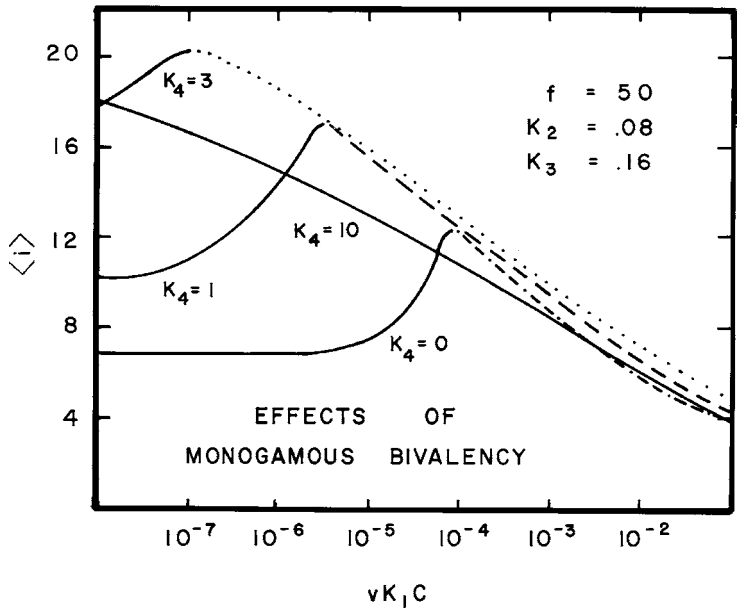

Fig. 4. Effects of monogamous bivalency on receptor aggregation The parameters generating these data were not intended to represent a specific cellular situation but rather to demonstrate qualitative features of the model. For the calculation shown, f and h are both 50, K_2 is 0.08, K_3 is 0.16 and K_4 is 1. The x-axis is the dimensionless reduced concentration vK_1c. The solid lines in the lower panel show $\langle i \rangle$ below the gel point for various values of K_4. Dotted lines indicate average size of sol-phase species *above* the gel points. The maximum amount of gel-phase ligand *decreases* with increasing K_4 and, for $K_4 = 10$, no gel point is observed.

maximum fraction of receptors involved in the gel decreases with increasing K_4. In the example shown, for K_4 equal to 0, 1 and 5, maximum amounts of 75, 60 and 11% of bound ligand are involved in gel-phase aggregates, respectively, while a value of $K_4 = 10$ inhibits gelation completely.

The receptor surface density S_0 exerts its effects *only* through the product K_2S_0 so that effect of changing receptor density is exactly equivalent to a corresponding increase in K_2 or K_3. Fig. 5 illustrates the relation between these binding constants and ligand valence. For large valences, receptor–antigen binding constants K_2 and K_3 and the corresponding antigen valences f and h effectively occur only as products with each other, as can be seen from examination of Eq. (8). Thus, doubling the ligand valence has almost, if not quite, the same effect as doubling the relevant binding constant. A valence of 50 is quite small in this context, but one can see that increasing f four-fold to 200 and decreasing K_2 by a similar factor produced almost no net change in the location of the critical point.

Finally, the quantity $r = K_3/K_2$ needs to be considered. This reflects the relative tendency of a ligand-bound receptor to bind to an available site on another bound ligand versus the tendency of a *free* receptor to attach to a bound ligand. Increasing values of r, thus, imply increasing tendency to form extended aggregates with large number of ligand–ligand receptor bridges. One might expect that r to be generally less than one [16]; however, as will be shown later, our photobleaching data suggest that this may not invariably be the case.

3.3. Biophysical results on receptor aggregation and gelation

Some of the most extensive data on aggregation of cell surface receptors by polyvalent ligand comes from immunology. The so-called Type 2 thymus-independent antigens are large polymers with repeating antigenic determinants. The biological effect of these antigens on antigen-specific cells, that is, cells whose BCR bind the haptenic determinant of the

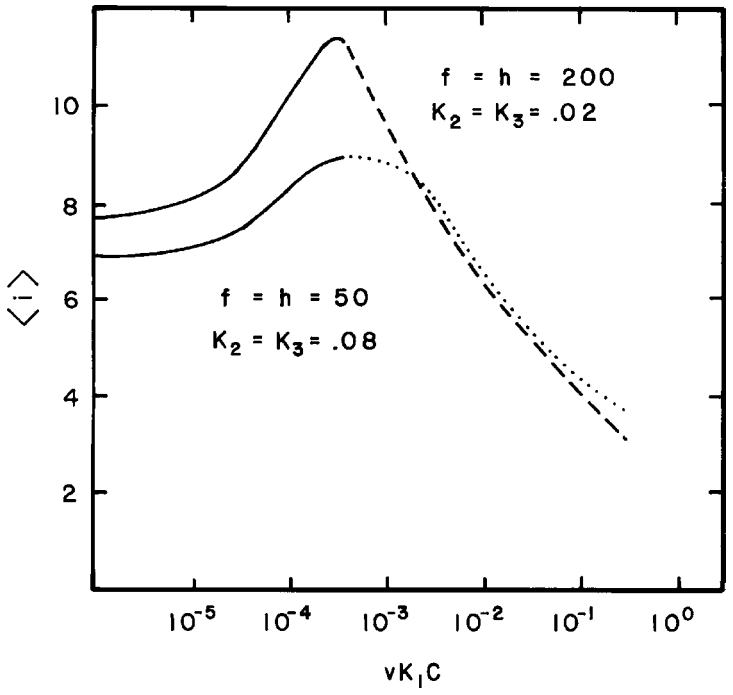

Fig. 5. Interrelation of f with K_2 and h with K_3. The parameters generating these data were not intended to represent a specific cellular situation but rather to demonstrate qualitative features of the model. Expansion of combinatorial expressions shows that f and K_2, like h and K_3, occur mainly as the product with each other. For the upper line, f and h are both 200 and K_2 and K_3 are 0.02. For the upper line, the product is the same, with f and h both 50 and K_2 and K_3 both 0.08. The x-axis is the dimensionless reduced concentration vK_1c. Aggregate sizes are grossly similar, the main difference being that the location of the gel point is affected somewhat by the absolute size of h so that the gel point for the f, $h = 200$ curve lies to the left of that for f, $h = 50$.

antigens, depend strongly on the antigen concentration and epitope density. Low concentrations and antigen valences cause cell differentiation while, for any given antigen epitope density, concentrations above some critical concentration cause first diminished cellular responses and then cell unresponsiveness even to other mitogens [15]. Fig. 6 shows this behavior for DNP–POL. Curves are labeled with the number of DNP groups per flagellin monomer. It is apparent that even a 50% change in antigen valence, from 2.3 to 3.5, produces a qualitative change in cellular response. Similar results have been observed for the additional TI-2 antigen DNP–dextran [20].

The B cell–DNP–POL system has been studied by fluorescence photobleaching recovery to measure lateral diffusion of BCR–antigen complexes for by various concentrations ands epitope densities of antigen [15]. In Fig. 7, the diffusion coefficient of a single BCR divided by the diffusion coefficient of bound antigen is plotted versus antigen concentration for several antigen epitope densities. As argued earlier [14], the diffusion constant of such aggregates would be inversely proportional to $\langle i \rangle$, the number of receptor molecules in the aggregate. Moreover, $\langle i \rangle$ could be found by dividing the diffusion constant of an isolated receptor by that of the aggregate. Thus, these data indicate that the size of mobile receptor–antigen aggregates increases both with antigen concentration and with epitope density. For higher epitope density antigens, when concentration exceeds a critical value, an additional immobile fraction of bound antigen, indicated by crosshatching, suddenly appears on the cell surface. This immobile ligand, coexisting with mobile antigen species, suggests the presence of a receptor–ligand gel. Again, DNP–dextran exhibits similar behavior in photobleaching experiments [20].

One might wonder whether such behavior could arise from specific phenomena peculiar to cell

Table 1
Sample parameters of divalent cell surface receptor aggregation by polyvalent ligand[a,b]

$\log_{10} C^*$	S/S_0	C_b	$\langle k \rangle$	$\langle i \rangle$	$\langle j \rangle$	M	g_s	g_g	S_g/S_0	C_g/C_b
−7	0.954	0.005	1.11	10.85	4.68	10.84	9.8	10.39	0	0
−6.5	0.899	0.011	1.26	11.98	5.14	12.66	9.49	10.03	0	0
−6	0.82	0.02	1.56	14.12	6.02	15.6	9.03	9.48	0	0
−5.5	0.727	0.032	2.04	17.22	7.27	18.57	8.43	8.79	0.01	0.037
5	0.634	0.047	2.04	15.69	6.66	17.96	7.68	8.05	0.101	0.268
−4.5	0.546	0.064	2.04	14.13	6.02	17.29	6.92	7.3	0.187	0.399
−4	0.462	0.085	2.04	12.55	5.35	16.56	6.14	6.54	0.267	0.481
−3.5	0.383	0.111	2.04	10.96	4.66	15.74	5.36	5.76	0.341	0.535
−3	0.309	0.144	2.05	9.39	3.96	14.86	4.58	4.98	0.409	0.571
−2.5	0.24	0.188	2.06	7.87	3.26	13.91	3.81	4.21	0.468	0.593
−2	0.178	0.248	2.1	6.47	2.6	12.94	3.08	3.46	0.517	0.602
−1.5	0.122	0.336	2.17	5.25	1.99	12.02	2.42	2.75	0.549	0.596
−1	0.076	0.463	2.34	4.32	1.46	11.29	1.84	2.11	0.552	0.564
−0.5	0.041	0.643	2.7	3.75	1.01	10.85	1.39	1.61	0.489	0.473
0	0.018	0.876	3.31	3.56	0.62	10.71	1.08	1.27	0.249	0.223
0.5	0.007	1.18	3.03	2.55	0.26	5.62	0.84	1.1	0	0
1	0.002	1.51	2.43	1.6	0.09	2.18	0.66	1.03	0	0
1.5	0	1.77	2.16	1.22	0.03	1.36	0.56	1	0	0
2	0	1.912	2.06	1.08	0.01	1.12	0.52	1	0	0

[a] Calculations providing data plotted in Fig. 2, namely for $f = h = 50$, $K_2 = 0.08$, $r = 2$ and $K_4 = 1$.

[b] Abbreviations: C^*, reduced ligand concentration (vK_1C); S/S_0, fraction free receptors; C_b, ligand bound per receptor; $\langle k \rangle$, average ligands per sol-phase aggregate; $\langle i \rangle$, average receptors per sol-phase aggregate; $\langle j \rangle$, average monogamous-bivalently bound receptors per sol-phase aggregate; M, mobility reduction index ($\langle ki \rangle / \langle k \rangle$); g_s, receptor–ligand ratio in sol; g_g, receptor–ligand ratio in gel; S_g/S_0, immobile (gel) fraction receptors; C_g/C_b, immobile (gel) fraction ligand.

membrane or internal cellular apparatus like cytoskeleton. Similar studies were conducted on cell-sized large unilamellar vesicles (LUV) into whose membranes were inserted approximately 150,000 DNP-specific monoclonal immunoglobulin molecules [10]. In this completely passive system, exactly the same photobleaching behavior was observed as with lymphocytes (Fig. 8). Aggregate sizes increased with increasing antigen concentration and epitope density for all systems studied. Most importantly, crosshatched areas indicate the observation of an immobile fraction of bound antigen coexisting with mobile species. It is important to note that this verification of gel formation is vividly apparent in the raw data and is not a product of data analysis.

This sudden appearance of immobile aggregates on completely fluid, homogeneous liposome surfaces is strikingly visible to the eye on photobleaching traces [10]. Fig. 9 shows FPR data of receptor complexes on liposomes with DNP–POL antigen of epitope density 3.5. Such liposomes are extremely fluid and devoid of calorimetric melting transitions. Thus, only by being anchored to a large number of membrane receptors could bound antigen appear immobile. The left-hand data trace shows 30% of immobile bound antigen in equilibrium with 70% of bound Ag diffusing freely with a diffusion coefficient of $1 \times 10^{-11}\,\mathrm{cm^2\,s^{-1}}$. Second and third bleaches at the same site (middle and right traces) eliminate the fluorescence contribution from immobile antigen so that the mobility of the diffusible species can more accurately be measured.

One can summarize by observing that optimum differentiation responses in B cells are induced by antigen treatment where bound antigen diffuses 6–15 times more slowly than individual BCR. However, high antigen concentrations and/or epitope densities induce formation of immobile bound antigen, the presence of which reduces or eliminates cell responses that would otherwise be expected. Comparing Figs. 6 and 7 suggest that optimum cell responses occur near the condition where immobile antigen first appears.

We must now ask whether *any* single set of model parameters can predict the sorts of aggregative phenomena observed or inferred from photobleaching

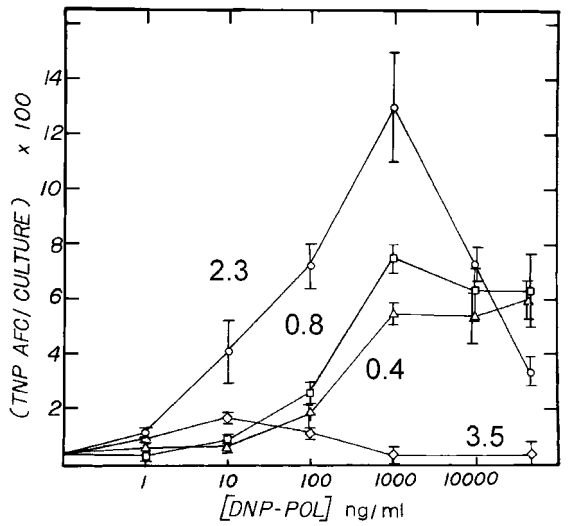

Fig. 6. In vitro immunogenicity for DNP–POL antigens as measured by direct hemolytic plaque assay. Cultures in the experiments consisted of 3,000,000 unfractionated mouse lymphocytes. Antibody forming cells are counted after 96 h stimulation. Epitope densities, i.e. DNP groups per 40,000 Da, are indicated beside each curve. Cells treated with concentrations of $DNP_{2.3}$–POL above $1\,\mu g\,ml^{-1}$ and all concentrations of $DNP_{3.5}$–POL were largely insensitive to subsequent antigenic or mitogenic challenge. Adapted from [15].

studies? An important and difficult constraint is that, at low antigen concentrations, bound antigen moves at a rate similar to individual BCR. This diffusion then slows at higher concentrations or epitope densities. This has strong implication for model parameters. Most simply, it means the product $K_2 f$ cannot be large. Otherwise antigen bound under any conditions will be attached to several receptors (see Fig. 1). However, gel formation, and indeed any substantial increase in aggregate size with ligand concentration such as we observe, requires a minimum ligand valence of 3. Thus, K_2 must be small. However, concentration-dependent increases in aggregate sizes require a substantial value for K_3. Thus, a value of r exceeding 1 seems inevitable.

If these steps are taken, then very attractive agreement between theory and experiment results. It seems plausible that, for geometric reasons, the actual valences f and h are fixed, for example, by lymphocyte surface irregularity. As the antigen epitope density increases, then the effect would be to correspondingly increase K_2 and hence also K_3. Fig. 10 shows the results of a calculation for $f = h = 3$, $r = 10$, $K_4 = 0$ and various values of K_2 covering a 10-fold range as

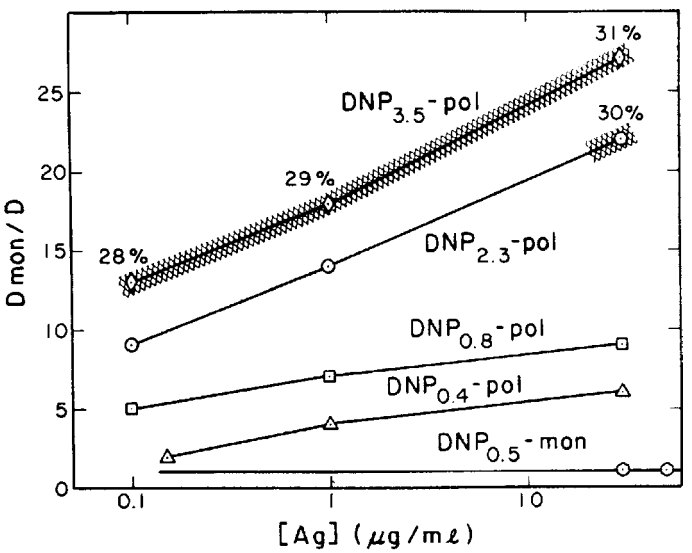

Fig. 7. Photobleaching recovery measurement of fluorescent DNP–POL antigen lateral diffusion on antigen-specific B cells. Mobility reduction indices (see text) for various epitope densities are plotted vs. antigen concentration. Shaded areas and percentile numbers indicate the presence and amount of an antigen-induced immobile fraction of BCR–antigen complexes *beyond* the immobile fraction normally observed for the BCR. Adapted from [15].

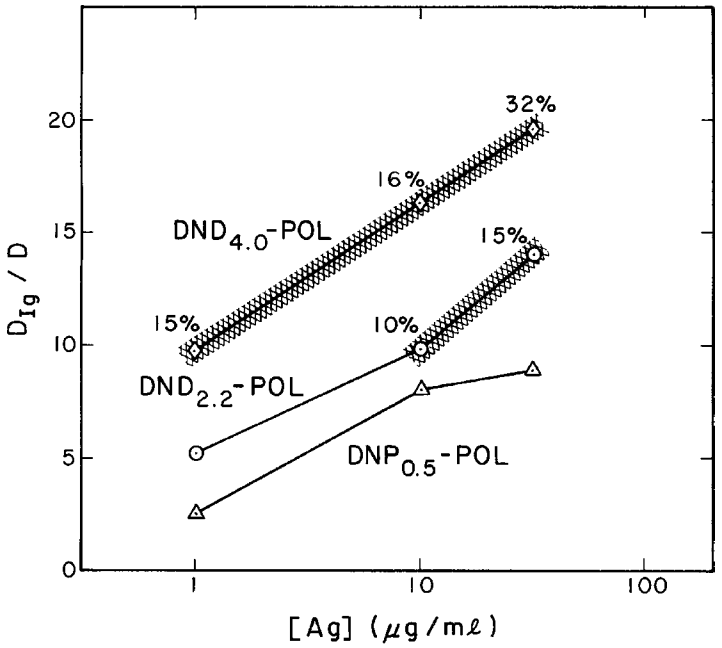

Fig. 8. Photobleaching recovery measurement of fluorescent DNP–POL antigen lateral diffusion on lymphocyte-sized liposomes bearing 150,000 DNP-specific artificial receptors. Mobility reduction indices (see text) for various epitope densities are plotted vs. antigen concentration. Shaded areas and percentile numbers indicate the presence and amount of an antigen-induced immobile fraction of artificial receptors. In the absence of polyvalent ligands, artificial receptors are 100% mobile. Adapted from [10].

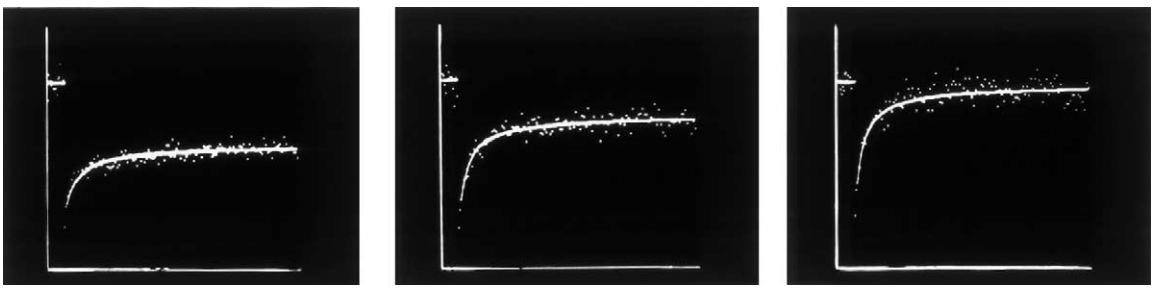

Fig. 9. Appearance of an immobile fraction of bound antigen on liposome bearing 150,000 DNP-specific artificial receptors and treated with 30 $\mu g\,ml^{-1}$ of DNP–4.0POL. Three sequential photobleaching traces of the same spot are shown. Each point is 200 ms; additional experimental details are give in [10]. The first bleach (left panel) shows >30% immobile antigen. By the third bleach (right panel), immobile antigen has been removed and fluorescence recovery is now 100% with same half-time as that exhibited by the mobile component at the start of the experiment.

did to our experimental data on DNP-specific B cells. The mobility reduction index $\langle ki\rangle/\langle k\rangle$ is plotted over the range of C^* corresponding to these photobleaching experiments. What we see is that mobility reduction indices predicting photobleaching results and reflecting aggregate sizes increase with antigen concentration. These increases occur at the same ligand concentrations and to the same approximate values inferred from both our cellular and our model liposome experiments. Critically, a gel-phase appears for the two higher epitope density antigens within the experimental range, but no gel appears for the lower epitope density antigens at any concentration, again as was observed experimentally. With the quantities

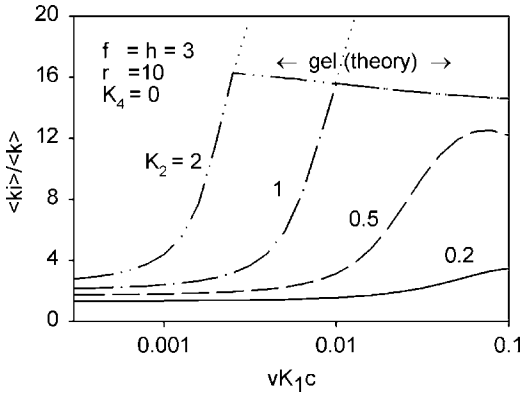

Fig. 10. Plots of mobility reduction indices vs. reduced antigen concentration calculated using parameters to give reasonable agreement with cellular (Fig. 7) and liposomal (Fig. 8) photobleaching recovery results. The model as presented here suggests that sol-phase aggregate sizes decrease slowly above the gel point (line marked "gel theory"). However, antigen heterogeneity such as definitely occurs with POL antigens would allow sol-phase species to grow above the gel point as shown by the dotted lines for $K_2 = 1$ and $K_2 = 2$ in a way corresponding to the crosshatched regions of Figs. 7 and 8.

used to generate Fig. 10, one sees that the theoretical gel point depends on K_2 in a way comparable to the dependence on epitope density shown in Figs. 6 and 7. According to our model, sol-phase aggregate sizes should remain approximately constant in size above the gel point. However, in a system with polydisperse antigen such as we certainly have [18], sol-phase aggregates would be expected to grow in size above the gel point as we observe experimentally and as the dotted lines above the gel points in Fig. 10 suggest.

4. Discussion

The computational technique described above provides a satisfactory method for calculating aggregate distributions produced by polyvalent ligands interacting with bivalent cell surface receptors. The principal point for discussion is the degree to which the model satisfactorily explains aspects of receptor aggregation which are observable on cell surfaces.

Generally, the model must be deemed successful. It predicts, for plausible values of the physical constants involved, a number of features observed experimentally. First, (mobile) aggregates involving relatively small numbers of receptors should form at low antigen concentration and epitope density as is observed in photobleaching studies on cells and liposomes. Second, arbitrarily large (gel-phase) aggregates should form at high antigen concentration and epitope density as is also observed clearly on liposomes. Third, total bound antigen is predicted to increase with antigen concentration and epitope density as is shown by flow cytometry. Fourth, the average mobile aggregate cannot involve more than two antigen molecules, thus, explaining the photobleaching observation that there is always a clear distinction between the mobile aggregates and the immobile fraction of gel-phase species. Finally, the step can be taken of fixing ligand valences f and h at small values and allowing r to exceed one, thus, encouraging ligand crosslinking of receptors. Once this is done, then something approaching quantitative agreement between photobleaching results and theory obtains (cf. Figs. 7 and 10).

Nonetheless, one can enumerate several points on which the model must necessarily break down to a greater or lesser degree. To assess how much any of these factors impacts on the physical realities of the systems studied is much more difficult. One problem is the existence of cyclic structures. These were explicitly excluded at the outset; however, this was for computational convenience and there is no a priori reasons why such entities should not exist. On the other hand, Goldberg has argued [3] that the contribution of cyclic aggregates should be small in the three-dimensional case. Since steric constraints are more severe in a two-dimensional system, it seems that cyclic aggregates on cell surfaces should be even less frequent. In any case, cyclic aggregate formation, like monogamous bivalency, competes with aggregate growth by branching and so reduces the numbers of ways by which gel-phase structures can form. This effect should increase strongly with ligand valence. As such, proper account of cyclization might reduce the overly strong ligand valence dependence of ligand concentration effects which the model currently predicts.

A second difficulty concerns the finiteness of the systems studied. While the mathematics assumes an infinite number of receptors, cells and liposomal models rarely express more than 10^5 copies of a given

receptor. This means that the hypothetical single huge aggregate which comprises the gel-phase cannot really exist. This also introduces the third way in which the model diverges from physical reality—the assumption of thermodynamic equilibrium. An arbitrarily large receptor–antigen aggregate would require an infinite time to form, simply from kinetic limitations on rates of receptor lateral diffusion. Both these factors should operate to favor smaller aggregates over gel under experimental conditions. Such effects are, however, difficult to gauge quantitatively. System finiteness might be dealt with by altering limits on the sums in the distribution function, but evaluation of the model under such constraints would be a major computational task. The kinetic question would be even more difficult to approach. The fact that photobleaching results on receptor-bearing liposomes do not vary with time of incubation with antigen [10] suggests that a state near equilibrium may be obtained with reasonable rapidity. On the other hand, Cohen and Benedek [21] have argued that kinetically-stable situations far from equilibrium can arise in systems capable of gelation. Thus, further investigation of this issue seems indicated.

The final difficulty with the model is the absence of allowance for polydispersity of antigen valence. Logically, one would expect the number of haptenic groups on a T-independent antigenic polymer to obey something approximating a Poisson distribution, so that antigen of any nominal valence would contain appreciable amounts of higher-valent material. Because the higher avidity of this fraction of antigen, it should be preferentially bound at equilibrium. Considered in a hypothetical limiting case, two epitope densities of antigen at the same concentration might be expected to behave as differing concentrations of the highest-valent material present in appreciable quantities. This would have the result of changing valence effects on the location of, say, critical points into concentration effects and, thus, diminishing the sensitivity of these locations to ligand valence. It is presently difficult to assess which if any of the above factors contribute to such quantitative discrepancies between theory and experiment as were noted at the beginning of Section 4.

In summary, we would suggest that gelation of B cell surface receptors under specific conditions of antigen concentration and valence is predicted by theory and demonstrated by experiment on both cell and model systems. It is known that conditions producing receptor ligand gel also produce a cellular state unresponsive to other antigenic and mitogenic challenge [15]. One can speculate how the such negative signals might be delivered by such extended receptor–ligand aggregates or “superaggregates” in the terminology of Goldstein and Perelson [16]. Extended aggregates might alter physical properties of the cell surface, non-specifically inhibiting receptor function. Alternatively, large structures might sequester accessory proteins essential to signaling by smaller, immmunogenic aggregates. Immobilized receptors might *excessively activate* some cell system, e.g. a protein kinase activity. Alternatively, we now know that BCR aggregates must translocate into lipid rafts to initiate their signaling cascade [22]. Give the extended nature of gel-phase aggregates, perhaps such large extensive structures might mechanically inhibit translocation of receptor-containing smaller aggregates to lipid rafts.

Acknowledgements

The author is especially grateful to Dr. Alan S. Perelson of Los Alamos National Laboratory for valuable advice concerning both the summation of the distribution function and treatment of two-dimensional gelation. Supported in part by NSF grant MCB 98-07822.

Appendix A. Derivation of W_{kij}

W_{kij} is the number of ways that i bivalent receptors and k polyvalent ligands can be assembled into a non-cyclic aggregate where j receptors are bound monogamous bivalently by both their valences to the same antigen molecule. The molecules and their combining sites are distinguishable and equivalent. The method of solving this problem in the absence of monogamous bivalency was put forward by Goldberg [3]. The following discussion represents an adaptation of his discussion, except that we have three ligand valences v, f, and h rather than just one, and the reader is referred to that article for additional detail. The ligands are taken to be “frames”, which can be

visualized as strips of sheet metal perforated by v holes in a line. Indistinguishable bolts long enough to penetrate two frames hold the frames together and also occupy all other holes. These latter bolts have a free end.

W_{kij} is the product of two terms: the number of ways W_k the k frames can be bolted together to using $k-1$ receptors to form an aggregate and the number of ways R_{kij} the remaining $i-k+1$ receptors can bind available ligand sites, j receptors being bound monogamous bivalently:

$$W_{kij} = W_k R_{kij} \tag{A.1}$$

Each of the k ligands must first bind a single receptor. This represent forming bonds of the first type and so can be done in

$$P = v^k \tag{A.2}$$

ways. These receptor-binding ligands are crosslinked into an aggregate for which only $k-1$ receptor are actually required. Any given final structure can be formed with the extra receptor located in any ligand valence not used to hold the final aggregate together. Thus, the P possible initial arrangements are actually D-fold degenerate in terms of generating specific aggregate structures where

$$D = fk - k + 1 \tag{A.3}$$

The relevant valence here is f since the Goldberg argument defining N actually discusses single ligands with all possible locations binding free receptors except one so that f is the correct valence for this situation. Finally, the k ligands with their initial receptors in place can be joined together in Q ways to give distinct aggregate structures plus one free receptor. This quantity is

$$Q = \frac{hk - k + 1}{hk - 2k + 2} \tag{A.4}$$

The final expression for W_k thus becomes

$$\begin{aligned} W_k &= \frac{PQ}{D} = \frac{v^k}{fk - k + 1} \frac{(hk - k + 1)!}{(hk - 2k + 2)!} \\ &= \eta(f, h, k) v^k \frac{(hk - k)!}{(hk - 2k + 2)!} \end{aligned} \tag{A.5}$$

The introduction of $\eta = (hk-k+1)/(fk-k+1)$ is necessary for practical summation of the distribution function. An approximation to this quantity satisfactory for most circumstances, namely $f = h$, $f \ll 1$ or $h \gg 1$, is $(h-1)/(f-1)$. Evaluation of R_{kij} follows straightforward combinatorial procedures. The particular method for treating monogamous bivalency of receptors was introduced by DeLisi and Perelson [12]. Of the i total receptors, $k-1$ are used to crosslink antigen molecules. The remaining $i-k+1$ receptors are divided into two groups, $q = i-k+1-j$ receptors singly-bound to antigen and j receptors monogamous bivalently bound to antigen. The q singly-bound receptors are to be distributed among $fk-2k+2-2j$ sites which remain free after the j monogamous bivalently bound receptors are located. This can be done in N_q ways where

$$N_q = \begin{pmatrix} fk - 2k + 2 - 2j \\ fk - 2k + 2 - 2j - q \end{pmatrix} \tag{A.6}$$

The j monogamous bivalently bound receptors can be located in $fk-2k+2-j$ possible locations, an arrangement possible in N_j ways where

$$N_j = \begin{pmatrix} fk - 2k + 2 - j \\ j \end{pmatrix} \tag{A.7}$$

The distribution of the i receptors among the various binding sites can take place in $i!$ ways. Because each receptor has two distinguishable valences, the i receptors can be attached in 2^i ways. R_{kij} is thus given by the expression

$$\begin{aligned} R_{kij} &= 2^i\, i! \frac{(fk - 2k + 2 - 2j)!}{(i - k + 1 - j)!(fk - k + 1 - j - i)!} \\ &\quad \times \frac{(fk - 2k + 2 - j)!}{j!(fk - 2k + 2 - 2j)} \end{aligned} \tag{A.8}$$

Replacing $i-k+1-j$ by q and $fk-2k+2$ by n yields the final value for W_{kij}

$$\begin{aligned} W_{kij} &= \eta\, i!\, v^k\, 2^i \frac{(hk - k)!}{(hk - 2k + 2)!} \frac{(n - j)!}{j!(n - 2j)!} \\ &\quad \times \frac{(n - 2j)!}{q!(n - 2j - q)!} \end{aligned} \tag{A.9}$$

This quantity can be substituted into Eq. (3) to yield the desired equilibrium constant K_{kij}.

Appendix B. Formula for $\sum iC_{kij}$

Evaluation of the sum is accomplished by differentiation of Eq. (15):

$$\sum iC_{kij} = S^* \frac{\mathrm{d}}{\mathrm{d}S^*} \sum C_{kij} = \frac{\eta S^*}{rK_2}[p' w_0 T_0(y_0) + p w_0' T_0(y_1) + p w_0 T_0'(y_0) + p' w_1 T_0(y_1) + p w_1' T_0(y_1) + p w_1 T_0'(y_1)] \quad \text{(B.1)}$$

where $p = (1+S^*)^2/S^*$, $w_0 = \xi/(1+\zeta)$, and $w_1 = \xi\zeta^3/(1+\zeta)$. In each case, the prime denotes differentiation with respect to S^*. Three of the derivatives are simply evaluated:

$$p' = \left(\frac{1}{S^*}\frac{S^*-1}{S^*+1}\right) p \quad \text{(B.2)}$$

$$w_0' = \left(\frac{\xi'}{\xi} - \frac{\zeta'}{1+\zeta}\right) w_0 \quad \text{(B.3)}$$

$$w_1' = \left(\frac{\xi'}{\xi} + \frac{3\zeta'}{\zeta} - \frac{\zeta'}{1+\zeta}\right) w_1 \quad \text{(B.4)}$$

where the intermediate quantities ξ' and ζ' being defined by

$$\xi' = \left[1 + \frac{1}{(1+4z)^{1/2}}\right] z' \quad \text{(B.5)}$$

$$\zeta' = \frac{z'\xi - \xi' z}{\xi^2} \quad \text{(B.6)}$$

Derivatives of the sums over k are evaluated by the chain rule. For example,

$$\frac{\mathrm{d}T_0(y_0)}{\mathrm{d}S^*} = \frac{\mathrm{d}T_0}{\mathrm{d}\alpha_0}\frac{\mathrm{d}\alpha_0}{\mathrm{d}y_0}\frac{\mathrm{d}y_0}{\mathrm{d}S^*} \quad \text{(B.7)}$$

Thus, the derivatives of the sums becomes:

$$T_0'(y_0) = \frac{1}{h(1-\alpha_0)^h} \times \left[\frac{1+S^*(f-1)}{S^*(1+S^*)} + \frac{f-2}{2}\frac{\xi'}{\xi}\right] y_0 \quad \text{(B.8)}$$

$$T_0'(y_1) = \frac{1}{h(1-\alpha_1)^h} \times \left[\frac{1+S^*(f-1)}{S^*(1+S^*)} + \frac{f-2}{2}\left(\frac{\xi'}{\xi} + \frac{2\zeta'}{\zeta}\right)\right] y_1 \quad \text{(B.9)}$$

These formulae, together with those in the text, provide complete information for the evaluation of $\sum iC_{kij}$ from Eq. (B.2). One must note that this sum, beginning at $k = 1$, does *not* include free receptors.

Appendix C. Formula for $\sum jC_{kij}$

Evaluation of the sum is accomplished by differentiation of Eq. (8):

$$\sum jC_{kij} = \frac{\eta(1+S^*)^2}{rK_2S^*} \sum_{k=1}^{\infty} \frac{(hk-k)!}{k!(hk-2k+2)!} \times [rC^*S^*(1+S^*)^{f-2}]^k z \frac{\mathrm{d}}{\mathrm{d}z} \times \sum_{j=0}^{\mathrm{int}(n/2)} \frac{(n-j)!}{j!(n-2j)!} z^j \quad \text{(C.1)}$$

When the inner sum is written in closed form and differentiated as indicated, there results will be as follows:

$$\sum jC_{kij} = z\left(\frac{\mathrm{d}z}{\mathrm{d}S^*}\right)^{-1} \frac{\eta(1+S^*)^2}{(rK_2S^*)} \left[\frac{f-2}{2}\frac{\xi'}{1+\zeta} T_1(y_0) + \frac{(1+\zeta)\xi' - \xi\zeta'}{(1+\zeta)^2} \times T_0(y_0) + \frac{f-2}{2}\frac{\zeta^3\xi' + 2\xi\zeta^2\zeta'}{1+\zeta} T_1(y_1) + \frac{(1+\zeta)\zeta^3\xi' + \zeta\xi^2(3+2\zeta)\zeta'}{(1+\zeta)^2} T_0(y_1)\right] \quad \text{(C.2)}$$

All the terms occurring in this equation have been defined either in the text or in the previous Appendices A and B.

References

[1] W.H. Stockmayer, Theory of molecular size distribution and gel formation in branched-chain polymers, J. Chem. Phys. 11 (1943) 45–55.
[2] J.E. Mayer, M.G. Mayer, Statistical Mechanics, Wiley, New York, 1940, pp. 1–456.
[3] R.J. Goldberg, A theory of antibody–antigen reactions. I. Theory for reactions of multivalent antigen with bivalent and univalent antibody, J. Am. Chem. Soc. 74 (1952) 5715–5725.

[4] A.S. Perelson, Some mathematical models of receptor clustering by multivalent ligands, in: A.S. Perelson, C. DeLisi, F.W. Wiegel (Eds.), Cell Surface Dynamics: Concepts and Models, first ed., Marcel Dekker, New York, 1984, pp. 223–276.
[5] C. DeLisi, Toward a dynamic theory of membrane organization and function, in: A.S. Perelson, C. DeLisi, F.W. Wiegel (Eds.), Cell Surface Dynamics: Concepts and Models, first ed., Marcel Dekker, New York, 1984, pp. 205–221.
[6] B. Baird, J. Erickson, B. Goldstein, P. Kane, A.K. Menon, D. Robertson, D. Holowka, Progress toward understanding the molecular details and consequences of IgE-receptor crosslinking, in: A.S. Perelson (Ed.), Theoretical Immunology. Part 1. SFI Studies in the Sciences of Complexity, Addison-Wesley, Reading, MA, 1988, pp. 41–59.
[7] B. Goldstein, R.G. Posner, D.C. Torney, J. Erickson, D. Holowka, B. Baird, Competition between solution and cell surface receptors for ligand. Dissociation of hapten bound to surface antibody in the presence of solution antibody, Biophys. J. 56 (1989) 955–966.
[8] B.G. Barisas, J.S. Peacock, Photobleaching recovery studies of antigen-specific mouse lymphocyte stimulation by DNP-conjugated polymerized flagellin, J. Supramol. Struct. Cell. Biochem. Suppl. 5 (1981) 263.
[9] B.G. Barisas, J.S. Peacock, Photobleaching recovery studies of antigen-specific mouse lymphocyte stimulation by DNP-conjugated polymerized flagellin, Biophys. J. 33 (1981) 195a.
[10] J.S. Peacock, B.G. Barisas, Photobleaching recovery studies of T-independent antigen mobility on antibody-bearing liposomes, J. Immunol. 131 (1983) 2924–2929.
[11] T.R. Londo, J.S. Peacock, D.A. Roess, B.G. Barisas, Lateral diffusion of antigen receptors artificially incorporated onto B lymphocytes, J. Immunol. 137 (1986) 1924–1931.
[12] C. DeLisi, A. Perelson, The kinetics of aggregation phenomena. I. Minimal models for patch formation on lymphocyte membranes, J. Theoret. Biol. 62 (1976) 159–210.
[13] H.W. Gould, Combinatorial Identities, Morgantown, WV, 1972, viii + 106 pp.
[14] B.G. Barisas, Photobleaching recovery studies of the mobility of polymeric antigens on B cell surfaces, in: A.S. Perelson, C. DeLisi, F.W. Wiegel (Eds.), Cell Surface Dynamics, Marcel Dekker, New York, 1984, pp. 167–202.
[15] J.S. Peacock, B.G. Barisas, Photobleaching recovery studies of antigen-specific mouse lymphocyte stimulation by DNP-conjugated polymerized flagellin, J. Immunol. 127 (1981) 900–906.
[16] B. Goldstein, A.S. Perelson, Equilibrium theory for the clustering of bivalent cell surface receptors by trivalent ligands: application to histamine release from basophils, Biophys. J. 45 (1983) 1109–1123.
[17] G.L. Ada, G.J.V. Nossal, J. Pye, A. Abbot, Behavior of active bacterial antigens during the induction of the immune response, Nature 199 (1963) 1257–1262.
[18] S.L. Woodard, M. Aldo-Benson, D.A. Roess, B.G. Barisas, Flow cytometric analysis of T-independent antigen binding to DNP-specific cells, J. Immunol. 155 (1995) 163–171.
[19] M. Dembo, B. Goldstein, Theory of equilibrium binding of symmetric bivalent haptens to cell surface antibody: application to histamine release from basophils, J. Immunol. 121 (1978) 345–353.
[20] J.S. Peacock, B.G. Barisas, Antigen-specific mouse lymphocyte stimulation by DNP-conjugated T-independent antigens studied by photobleaching recovery, J. Supramol. Struct. Cell. Biochem. 17 (1981) 37–49.
[21] R.J. Cohen, G.B. Benedek, Equilibrium and kinetic theory of polymerization and the sol–gel transition, J. Phys. Chem. 86 (1986) 3696–3714.
[22] M.L. Dykstra, A. Cherukuri, S.K. Pierce, Floating the raft hypothesis for immune receptors: access to rafts controls receptor signaling and trafficking, Traffic 2 (2001) 160–166.